

Chapter-VI

Formation, thermodynamic properties, microstructures and antimicrobial activity of mixed cationic/non-ionic surfactant microemulsions with isopropyl myristate as oil

Abstract: *Hypothesis:* Modification of the interface by blending of surfactants produces considerable changes in the elastic rigidity of the interface, which in turn affects the physicochemical properties of w/o microemulsions. Hence, it could be possible to tune the thermodynamic properties, microstructures and antimicrobial activity of microemulsions by using ionic/non-ionic mixed surfactants and polar lipophilic oil, which are widely used in biologically relevant systems.

Experiments: The present report was aimed at precise characterization of mixed cetyltrimethylammonium bromide and polyoxyethylene (23) lauryl ether microemulsions stabilized in 1-pentanol (Pn) and isopropyl myristate at different physicochemical conditions by employing phase studies, the dilution method, conductivity, DLS, FTIR (with HOD probing) and ^1H NMR measurements. Further, microbiological activities at different compositions were examined against two bacterial strains *Bacillus subtilis* and *Escherichia coli* at 303K.

Findings: The formation of mixed surfactant microemulsions was found to be spontaneous at all compositions, whereas it was endothermic at equimolar composition. FTIR and ^1H NMR measurements showed the existence of bulk-like, bound and trapped water molecules in confined environments. Interestingly, composition dependence of both highest and lowest inhibitory effects were observed against the bacterial strains, whereas similar features in spontaneity of microemulsion formation were also evidenced. These results suggested a close relationship between thermodynamic stability and antimicrobial activities. Such studies on polar lipophilic oil derived mixed surfactant microemulsions have not been reported earlier.

Keywords: Mixed microemulsion, Interfacial composition; Polar lipophilic oil; Thermodynamic parameter; Droplet dimension; Percolation; Water state; Synergism; Antimicrobial activity.

1. Introduction

Microemulsions are optically isotropic and thermodynamically stable nanosized structured mixtures of water, oil, and amphiphile(s). They usually contain cosolvents or cosurfactants to achieve the low interfacial tension. Upon water dilution, three major structural domains can be distinguished: water-in-oil (w/o), bicontinuous, and oil-in-water (o/w) [1]. W/o microemulsions are made up of droplets of water surrounded by an oil continuous phase. These are generally known as “reverse micelles” (RMs), where the polar head groups of surfactant are facing into the droplets of water, with the hydrophobic tails facing into the oil phase. In the RMs, the amount of water present is low and is limited to the maximum capacity of hydration of the hydrophilic head group of the surfactants; hence, the water pool is rigid. In a w/o microemulsion, when the amount of water exceeds the hydration requirement of the surfactant head groups, both bound and free water prevail in the water pool. A term ω defined as water-to-surfactant molar ratio ($[\text{water}]/[\text{surfactant}]$) has been taken as a criterion as to whether a RM or a w/o microemulsion has been formed [2]. It was suggested that when $\omega < 10$, it is a RM and when $\omega > 10$, it is a w/o microemulsion [3]. However, some evidence exists that the cut-off point may be $\omega = 15$ [4]. However, in our previous report detailed introductory discussion on the basic aspects viz. formation characteristics, properties and structural characterization of microemulsions and RMs stabilized by single and mixed surfactants in nonpolar, polar and biocompatible oils was presented [5].

Further, the previous report delineated the phase characteristics, interfacial composition, thermodynamics of alkanol transfer process, transport properties and microstructure of water/mixed anionic (sodium dodecylsulfate, SDS) and nonionic [polyoxyethylene (23) lauryl ether, Brij-35]/1-pentanol (Pn)/isopropyl myristate, IPM (polar lipophilic oil) microemulsions under different physicochemical conditions, by employing the dilution method, conductivity and dynamic light scattering (DLS) measurements [5]. In view of the above, the present report aims at a precise characterization of the molecular interactions among the constituents, and enlightens the formation vis-à-vis nature of the oil/water interface in the microenvironment of mixed cationic (cetyltrimethylammonium bromide, CTAB) and nonionic (Brij-35) microemulsions stabilized in Pn and IPM as a function of ω , composition (mole fraction of nonionic surfactant in mixed surfactant

system, X_{nonionic}), and temperature, and comparison of the results in the light of changes in size and type of polar head group of basic surfactants (viz. CTAB with CTA^+ and SDS with DS^-) as well as unequal hydrocarbon chain lengths of CTAB (C_{16}) and Brij-35 (C_{12}). Justification of using Pn as cosurfactant and IPM as oil phase has been discussed in our previous report [5]. The present report sheds on the formation and composition of mixed interfacial film, complete analysis of thermodynamics of the transfer process of cosurfactant from bulk oil to the interface, transport property and microstructure of these systems by means of phase study, the dilution method, conductivity, and DLS measurements. The dilution experiment based on titrimetric method was pioneered by Bowcott et al. [6]. Later on, Palazzo et al. [7] pointed out that the method has applications in scattering and diffusion studies, because it provides extrapolation to single-particle properties by reducing inter-particle interactions of the microemulsion system without changing its composition. Knowledge on the state of solubilized water is important because this sustains the applications of these species viz. in solubilization, catalysis of chemical reactions [8, 9] and also in size and polydispersity of nanoparticles synthesized in the microemulsion [10]. The different states of solubilized water were characterized by employing several techniques [11-17]. Most of the studies on the structure of the water solubilized in reverse aggregates are reported using two noninvasive techniques, proton nuclear magnetic resonance (^1H NMR) and Fourier transform infrared spectroscopy (FT-IR) [11-14, 16]. Hence, the physicochemical properties of solubilized water have been determined using FTIR (with HOD probing) and ^1H NMR spectroscopic measurements. Attempt has been made to shed light on the effects of the molecular structure of the mixed surfactants and polar lipophilic oil (which is structurally and physicochemically different from hydrocarbon oil) on the state of water in the pool of the present system. Reports are available in literature that microemulsions are membrane-active, antimicrobial, self-preserving in their own right [18]; as bacteria cannot survive in pure fat or oil, whereas water is necessary for their growth and reproduction [19]. Recently, a few reports on the use of microemulsions as food-grade antimicrobial agents suggested that there may be a link between the antimicrobial activity of microemulsions and their overall stability [20-23]. Further, it has been suggested that the molecular and ionic structure of liposome is harmful to the

bacterial cell and in particular, that they adversely affect the structure and function of the bacterial membrane [24]. To the best of our knowledge, such studies employing mixed surfactant microemulsions in IPM have not been reported earlier. Therefore, augmenting the relationship between the physicochemical and thermodynamic properties of the microemulsions and their antimicrobial activity is necessary. Hence, antimicrobial activity or inhibitory effect of the microemulsions systems against the strains gram-positive - *Bacillus subtilis* (*B. subtilis*) and gram-negative - *Escherichia coli* (*E. coli*) bacteria has been examined in individual constituents and also at different compositions of mixed surfactants [$X_{\text{Brij-35}} = 0.0 \rightarrow 1.0$, S/CS = 1:2 (w/w)] of microemulsions at 303K, by measuring the diameter of the inhibition zone (“diz”). A correlation between composition dependence of antimicrobial activity and stability of these systems has been reported. Moreover, overall results of this report would be helpful in better understanding of mixed surfactant derived microheterogeneous systems in polar lipophilic oil.

2. Experimental

2.1. Materials

Cetyltrimethylammonium bromide (CTAB, $\geq 99\%$) and polyoxyethylene (23) lauryl ether (Brij-35, $\geq 99\%$) were purchased from Sigma Aldrich, USA. The oil, isopropyl myristate (IPM, $\geq 98\%$) and the alkanol, 1-pentanol (Pn, $\geq 98\%$) were products of Fluka, Switzerland. Deuterium oxide (D_2O , ≥ 99.8) was the product of Acros Organics, USA. The dye, methylene blue (MB, $> 99\%$), was a product of Merck, Germany. All these chemicals were used without further purification. Doubly distilled water of conductivity less than $3 \mu\text{S cm}^{-1}$ was used in the experiments. Bacterial strains used in this study were procured from Institute of Microbiology Technology, Chandigarh. *Bacillus subtilis* (MTCC No-2358) (gram positive) and *Escherichia coli* (MTCC No-2939) (gram negative) were used for examining antibacterial properties, and both these species were grown in nutrient agar media (pH 7.0) (HiMedia Pvt. Ltd., Mumbai, India).

2.2. Methods

2.2.1. Construction of pseudo ternary phase diagram of microemulsions

Pseudo-ternary phase diagram was constructed to find out the concentration range of all components (oil/water/surfactant and/or cosurfactant) in which they form microemulsion. The phase diagram was constructed by titrimetric method at ambient temperature.

Mixture of oil (IPM) and surfactant (CTAB and Brij-35) was prepared in different weight percentages keeping 1:2 ratio of surfactant to cosurfactant (Pn). The mixture was titrated drop-wise with water under gentle magnetic stirring and was sonicated for 10 minutes. The samples were classified as microemulsions when they appeared as clear transparent and translucent liquids and the respective solutions were left for overnight to make sure that there is no phase separation. After being equilibrated, the systems were visually characterized. The accuracy in the location of the phase boundaries was within 4 wt %.

2.2.2. Characterization of microemulsions

Dilution experiment

The dilution method is accomplished by adding oil at a constant water and surfactant level to destabilize an otherwise stable w/o microemulsion and then restabilizing it by adding a requisite amount of cosurfactant (alcohol) with constant composition of interface and continuous phase. The procedure of this experiment at different physicochemical conditions with theoretical backgrounds (i.e., basics of the dilution method and evaluation of thermodynamic parameters) were presented in our previous reports [5, 25, 26]. However, the essential equations concerning the evaluation of thermodynamic parameters are as follows, $\Delta G_t^0 = -RT \ln K_d$ (1)

where, K_d and ΔG_t^0 represent the distribution constant of alkanol and the standard Gibbs free energy change of transfer of alkanol from oil to the interface, ($P_{n_{oil}} \rightarrow P_{n_{int}}$).

ΔH_t^0 (enthalpy change of transfer of alkanol from oil to the interface) can be evaluated by the van't Hoff equation. Thus, $[\partial(\Delta G_t^0/T)/\partial(1/T)]_p = \Delta H_t^0$ (2)

Since the dependency of $(\Delta G_t^0/T)$ on $(1/T)$ are nonlinear for all these systems, a two-degree polynomial equation of following form is used. A representative nonlinear plot between $(\Delta G_t^0/T)$ on $(1/T)$ for water/CTAB/1-pentanol/IPM system has been provided in Appendix D (Fig. S1), whereas other figures are not exemplified.

$$(\Delta G_t^0/T) = A + B_1(1/T) + B_2(1/T)^2 \quad (3)$$

The differential form of the relation helps to evaluate ΔH_t^0 . Thus,

$$\partial(\Delta G_t^0/T)/\partial(1/T) = B_1 + 2B_2(1/T) = \Delta H_t^0 \quad (4)$$

where, A, B₁ and B₂ are the polynomial coefficients.

Then the Gibbs-Helmholtz equation is used to evaluate ΔS_t^0 (entropy change of transfer of alkanol from oil to the interface), $\Delta S_t^0 = (\Delta H_t^0 - \Delta G_t^0)/T$ (5)

The evaluation of specific heat change of transfer of alkanol from oil to the interface $[(\Delta C_p^0)_i]$ follows from the relation, $[(\Delta C_p^0)_i] = (\partial \Delta H^0 / \partial T)_p$ (6)

The standard state herein considered is the hypothetical ideal state of the unit mole fraction.

Conductivity measurement

The electrical conductivity was measured using Mettler Toledo (Switzerland) Conductivity Bridge. The instrument was calibrated with standard KCl solution. The temperature was kept constant (303K) for conductivity measurement within $\pm 0.01^\circ\text{C}$ by circulating thermostated water, through a jacketed vessel containing microemulsion. The reproducibility of the conductivity measurement was found to be within $\pm 1\%$.

Dynamic light scattering (DLS) measurement

The size of the microemulsion droplet was determined from DLS measurement. The same set of solution, as used in the conductance measurements, was employed for droplet size analysis at 303K. DLS measurements were carried out using a Zetasizer Nano ZS90 (ZEN3690, Malvern Instruments Ltd, U.K.). A He-Ne laser of 632.8 nm wavelength was used and the measurements were made at a scattering angle of 90° . Details of the measurement were presented in Mitra et al. [16], Bardhan et al. [26].

Spectroscopic measurements

FTIR spectra were recorded on a Perkin Elmer Spectrum RXI spectrometer (USA) (Absorbance mode) using a CaF_2 -IR crystal window (Sigma-Aldrich) equipped with a Presslock holder with 100 number scans and spectral resolution of 4 cm^{-1} . Deconvolution of spectra has been made with the help of Gaussian curve fitting program (Origin software). ^1H NMR spectra were recorded on a Bruker spectrometer (Germany) operating at 25°C . The instrument was operated at a frequency of 300 MHz. Calibration of proton chemical shift was measured relative to internal tetramethylsilane, TMS as reported earlier [14, 27].

2.2.3. Antimicrobial activity assay

The antimicrobial activity of individual constituents (surfactants, cosurfactant and oil) as well as the mixed surfactant microemulsion formulations was measured by employing the method of diffusion disc plates on agar [28, 29]. 28 gm of nutrient agar media was suspended in 1000 ml of distilled water according to the manufacturer's protocol. It was

boiled to dissolve the medium completely at sterilized condition by autoclaving at 15 lbs pressure (121°C for 15 minutes). The nutrient agar contained peptic digest of animal tissue (5 gm), sodium chloride (5 gm), beef extract (1.5 gm), yeast extract (1.5 gm), agar (15 gm) and was dissolved in water (1000 ml) and pH was adjusted to 7.0. The inoculum was freshly prepared in nutrient broth for 24 hours. The respective inoculum (100 μ l) with approximately 10^8 bacteria per milliliter was spread all over the surface of nutrient agar plate using glass spreader. Subsequently, the sterile Whatman filter paper discs (6 mm diameter) were soaked in microemulsion systems of different compositions with the variation of $X_{\text{Brij-35}}$ (= 0, 0.2, 0.4, 0.5, 0.6, 0.8, and 1.0) and were placed on agar plate. The diameters of the inhibition zones (diz/mm) were determined after incubation at 303K for 24 hours and compared with both surfactants, cosurfactant and oil alone. All tests were made in triplicates. The inhibition zones were measured using scale. Further, the diffusion of the microemulsion systems has been examined in the media (nutrient agar) by the dye encapsulation method at 303K for 24 hours.

3. Results and Discussion

3.1. Phase behavior of single and mixed surfactant microemulsions

CTAB/Brij-35: 1-pentanol

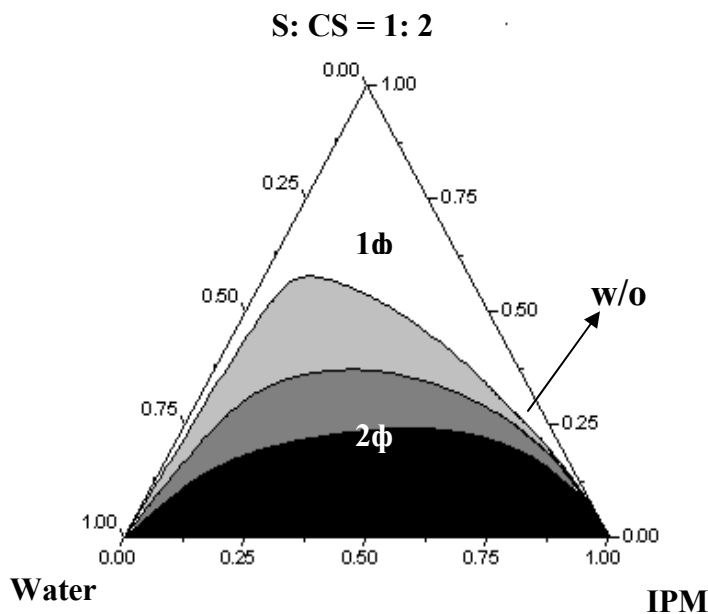


Fig. 1. Representative pseudo-ternary phase diagram of water/CTAB/Brij-35/Pn/IPM w/o microemulsion at three different ratios of mixed surfactant at 303K. S/Cs mass ratio: 1:2.

Area marks: unshaded, microemulsion zone (1 ϕ); shaded, turbid zone (2 ϕ) [black; $X_{\text{Brij-35}} = 0.0$, dark gray; $X_{\text{Brij-35}} = 0.5$, light gray; $X_{\text{Brij-35}} = 1.0$]. Appearance of viscous and other phases along the [surfactant(s): cosurfactant/water]-oil axis have not been shown for simplicity.

Phase diagram of pseudo-quaternary system, water/CTAB/Brij-35/Pn/IPM has been constructed in Gibbs triangle with varying content of Brij-35 ($X_{\text{Brij-35}} = 0.0, 0.2, 0.4, 0.5, 0.6, 0.8, 1.0$) at a fixed amount of mixed surfactant (CTAB/Brij-35) and constant temperature of 303K (illustrative representation has been shown in Fig. 1 at $X_{\text{Brij-35}} = 0, 0.5$ and 1.0, other figures are not exemplified here). The surfactant and cosurfactant ratio used was 1:2 (w/w). Along with cosurfactant (Pn), CTAB/Brij-35 (mixed surfactants) has been found to favorably augment microemulsification (1 ϕ region) of water and IPM. The findings and the discussions on the phase behavior are presented in Appendix D (Sec. 1).

3.2. Interfacial composition and stability of single and mixed surfactant microemulsions

Understanding of the interfacial cosurfactant and surfactant compositions as well as the distribution of the cosurfactant between the interface and the oil in different physicochemical conditions can quantitatively account for the thermodynamic stability of microemulsion on the basis of dilution experiment (described in the Sec. 2.2.2) and is presented as follows:

3.2.1. Effect of $X_{\text{Brij-35}}$ and temperature on interfacial (n_a^i) and bulk oil (n_a^o) compositions of Pn

The dilution method has been employed for evaluation of the interfacial composition of water/CTAB/Brij-35/Pn/IPM microemulsion systems as a function of composition ($X_{\text{Brij-35}} = 0, 0.2, 0.4, 0.5, 0.6, 0.8$ and 1.0) and temperature (viz. 293, 303, 313 and 323K) at fixed $\omega = 20$. From the data collected, graphs were constructed by plotting n_a^i/n_s vs n_o/n_s according to Eq. (S1) where n_s , n_a and n_o represent the total number of moles of surfactant, alkanol and oil respectively (Appendix D, Sec. 2). Representative illustrations are shown in Fig. S2 (Appendix D). The plots were strikingly linear [average correlation coefficient (R^2) was 0.9987].

Table 1. Temperature and surfactant composition dependent thermodynamic parameters for the formation of w/o mixed surfactant microemulsion in IPM at fixed water content ($\omega = 20$).
a,b

$X_{\text{Brij-35}}$	T/K	$10^4 n_a^i$ (mol)	$10^3 n_a^o$ (mol)	$-\Delta G_t^0$ (kJmol ⁻¹)	ΔH_t^0 (kJmol ⁻¹)	ΔS_t^0 (JK ⁻¹ mol ⁻¹)
0.0	293	11.75	5.88	2.08	-0.13	6.67
	303	12.94	5.77	2.26	-5.49	-10.66
	313	13.70	3.85	2.53	-11.04	-27.16
	323	19.51	3.43	3.07	-16.76	-42.39
0.2	293	17.96	4.72	2.12	-3.20	-3.73
	303	18.09	4.49	2.31	-6.78	-14.75
	313	21.13	3.38	2.82	-10.48	-24.49
	323	23.70	3.26	3.27	-14.29	-34.17
0.4	293	19.21	4.75	2.21	-4.25	-6.98
	303	22.42	4.48	2.46	-5.45	-9.86
	313	23.51	3.59	2.98	-6.68	-11.83
	323	31.93	3.43	3.32	-7.95	-14.34
0.5	293	12.94	8.87	1.05	17.54	63.46
	303	17.23	7.08	1.59	11.58	43.47
	313	20.01	6.23	1.92	5.42	23.46
	323	21.26	6.07	2.06	-0.94	3.47
0.6	293	15.15	6.18	1.66	30.20	108.75
	303	24.43	5.55	2.68	17.09	65.26
	313	25.68	3.69	2.96	3.53	20.76
	323	28.99	3.68	3.10	-10.45	-22.75
0.8	293	20.24	5.44	2.01	-2.08	-0.21
	303	20.43	5.12	2.19	-2.67	-1.59
	313	21.62	4.91	2.36	-3.29	-2.96
	323	22.35	4.59	2.58	-3.93	-4.17
1.0	293	17.33	5.86	1.82	0.72	8.67
	303	17.89	5.59	1.97	-5.24	-10.77
	313	26.77	5.55	2.25	-11.39	-29.23
	323	27.30	4.27	2.80	-17.76	-46.31

^a All the mixed microemulsion systems are formed using constant amount of mixed surfactant (0.5mmol) and oil (14.0 mmol). ^b The error limits in K_d , ΔG_t^0 , ΔH_t^0 and ΔS_t^0 are $\pm 1\%$, $\pm 3\%$, $\pm 5\%$ and $\pm 8\%$, respectively.

The calculated values of number of moles of alkanol in the interface (n_a^i) and oil phase (n_a^o) obtained at different compositions ($X_{\text{Brij-35}} = 0 \rightarrow 1.0$) with varying temperature (293-323K), are presented in Table 1. It is evident from Table 1 that the values of n_a^i and n_a^o did not follow any straightforward trend as a function of $X_{\text{Brij-35}}$ for any of these systems at the studied temperature range. Further, it is evident from the Table 1 that with increase in temperature n_a^i increases, while n_a^o decreases with increasing temperature and hence, increase in temperature helps to transfer more Pn molecules (cosurfactant) from the oil to the interface. This observation is found to be consistent with that reported earlier for single (of different charge types) and mixed surfactant microemulsions comprising both hydrocarbon oils and IPM [5, 30, 31]. When CTAB and Brij-35 are mixed at an equimolar composition or in the vicinity of it (that is, $X_{\text{Brij-35}} = 0.4 \rightarrow 0.6$), the difference between the values of n_a^i and n_a^o at lower and higher temperatures are more than the pure surfactant systems ($X_{\text{Brij-35}} = 0$ and 1.0). It indicates that interfacial arrangements or organizations of the constituents at the interface are mostly affected by increase in temperature in the vicinity of equimolar composition. Similar observation was also reported for mixed anionic/nonionic (SDS/Brij-35) systems stabilized in Pn and IPM [5].

3.2.2. Thermodynamics of transfer of alkanol (Pn) from oil (IPM) to the interface

In this section, thermodynamic parameters, the standard Gibbs free energy (ΔG_t^0), enthalpy (ΔH_t^0), entropy (ΔS_t^0) and specific heat capacity [$(\Delta C_p^0)_t$] for the transfer of Pn from the continuous oil phase (IPM) to the interfacial region of mixed surfactants (CTAB/Brij-35), ($\text{Pn}_{\text{oil}} \rightarrow \text{Pn}_{\text{int}}$) with varying ω ($= 20, 25, 30, 35, 40$ and 45) at an equimolar composition ($X_{\text{Brij-35}} = 0.5$) and temperature (303K) and also at a fixed ω ($= 20$) with varying both $X_{\text{Brij-35}}$ ($= 0 \rightarrow 1.0$) and temperatures (293, 303, 313 and 323 K) have been evaluated according to Eqs. (3-8). The data are presented in Table S1 and Table 1. Representative plots of $-\Delta G_t^0$ vs. $X_{\text{Brij-35}}$ and ΔH_t^0 or ΔS_t^0 vs. $X_{\text{Brij-35}}$ for water/CTAB/Brij-35/Pn/IPM system at four different temperatures are illustrated in Fig. 2, Figs. S3A and S3B, respectively. It is evident from Fig. 2, Table 1 and Table 2 that ΔG_t^0 values are negative at all compositions ($X_{\text{Brij-35}} = 0 \rightarrow 1.0$), water contents (ω) and temperatures in IPM, hence spontaneous formation of w/o microemulsions is suggested. Both similar and dissimilar trends in all these energetic parameters at comparable physicochemical environments are reported [31-33]. The deciphering of different

phenomena that guide the overall thermodynamics of the transfer of Pn to the interface is worthwhile but complex. However, an attempt has been made to present a comprehensive views based on the experimental results.

Table 2. Water content (ω) and cosurfactant dependent physicochemical parameters for the formation of w/o mixed microemulsion at fixed $X_{\text{Brij-35}}$ (0.5) and temperature (303K).
a, b

System: water/CTAB+Brij-35/Pn/IPM						
ω	20	25	30	35	40	45
$10^4 n_a^1/\text{mol}$	18.09	19.55	20.34	24.67	22.02	19.94
$10^3 n_a^0/\text{mol}$	10.46	13.94	15.11	19.61	21.93	22.66
K_d	1.82	1.58	1.53	1.41	1.33	1.28
$-\Delta G_t^0/\text{kJ mol}^{-1}$	1.51	1.16	1.08	0.88	0.71	0.63

^a All the mixed microemulsion systems are formed using constant amount of mixed surfactant (0.5 mmol) and oil (14.0 mmol). ^b The error limits in K_d and ΔG_t^0 are $\pm 1\%$ and $\pm 3\%$, respectively.

Effect of ω on ΔG_t^0 of transfer process

It is evident from Table 2 that the values of $-\Delta G_t^0$, which is indicative of spontaneity of the alkanol transfer process ($\text{Pn}_{\text{oil}} \rightarrow \text{Pn}_{\text{int}}$), decrease with increasing ω (= 20 to 45) for the mixed microemulsion systems. Similar trend of transferring of cosurfactant from oil to the interface and vice versa was discussed for single and mixed surfactant microemulsions by Bardhan et al. [5], Kundu et al. [25], Paul and Nandy [30], Hait and Moulik [31]. Further, it can be observed from Table 2 that, spontaneity of the alkanol transfer process ($\text{Pn}_{\text{oil}} \rightarrow \text{Pn}_{\text{int}}$) for mixed (CTAB/Brij-35) systems is higher compared to mixed (SDS/Brij-35) systems (-1.41 to -0.61 kJ mol⁻¹ at $\omega = 20$ to 40) at comparable physicochemical conditions in IPM [5]. The ionic surfactant with longer hydrocarbon chain (herein, CTAB) possesses higher efficiency to change the hydrophilicity and makes the interfacial layer effectively more hydrophobic irrespective of charges of ionic head

group [26]. Also, the larger bending elastic modulus of the interfacial layer arising out of the longer chain of the ionic surfactant, leads to larger solubilization ability [34]. These two effects determine the higher efficiency of ionic surfactant with longer hydrocarbon chain to form w/o microemulsions [35]. Hence, the effective binding between Pn and CTAB or SDS/Brij-35 at the interface increases in the order: SDS/Brij-35 < CTAB/Brij-35, which corroborates well with the degree of spontaneity of the transfer process. Similar observation is also reported earlier by Bera et al. [34] for water/SDS or CTAB/3-methyl-1-butanol/hydrocarbon oil (C₆-C₁₂) microemulsion systems.

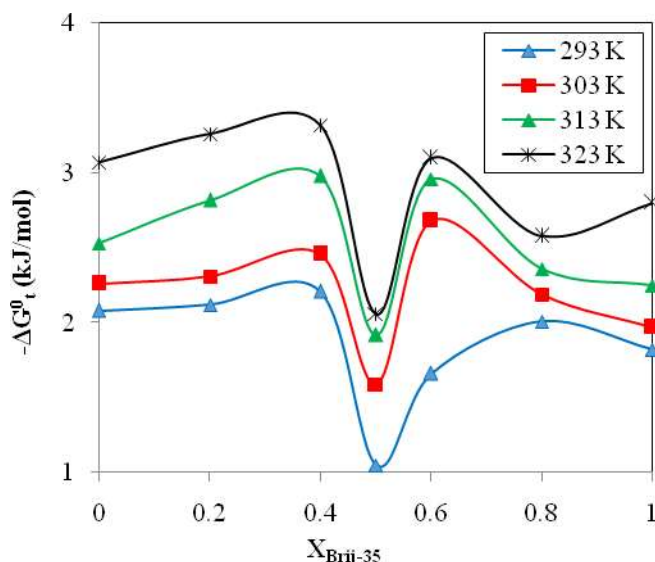


Fig. 2. Standard free energy change of transfer ($-\Delta G_t^0$) against composition ($X_{\text{Brij-35}}$) for w/o microemulsion systems comprising 0.5 mmol of mixed surfactant (CTAB/Brij-35) and 14.0 mmol of IPM oil stabilized by Pn at fixed water content ($\omega = 20$) with varying temperature (293K→323K).

Effect of X_{nonionic} and temperature on ΔG_t^0 of the transfer process at a fixed ω

It can be seen from Table 1 that the spontaneity of the transfer of Pn from oil (IPM) to the interface ($\text{Pn}_{\text{oil}} \rightarrow \text{Pn}_{\text{int}}$) for single CTAB or Brij-35 stabilized system increases with increase in temperature. This trend for single CTAB derived system corroborates well with the results reported earlier for CTAB or CTAC derived system stabilized in hydrocarbon, IPM and diesel oils [31, 34, 36, 37] and CTAB-[bmim][BF₄] system in toluene [38]. The trend of spontaneity of single Brij-35 derived system in IPM agrees well with previous reports [32, 39]. Further, it is evident from Table 1 and representative

plot of $-\Delta G_t^0$ vs. $X_{\text{Brij-35}}$ at four temperatures in IPM (depicted in Fig. 2) that the ΔG_t^0 values are not straightforward at mixed compositions (i.e. $X_{\text{Brij-35}} = 0.2 - 0.8$). $-\Delta G_t^0$ values increase with increase in temperature (293, 313 and 323 K) at all compositions for all these systems.

Further, it has been observed that $-\Delta G_t^0$ values of mixed CTAB/nonionic/Pn system stabilized in IPM are small compared to the values obtained in our previous reports for CTAB/nonionic/Pn and SDS/nonionic/Pn systems in hydrocarbon oils (Hp and Dc) under comparable physicochemical environments [26, 32, 33]. This can be explained in the following way. IPM, being amphiphilic polar oil, is not solubilized in the palisade layer, rather than it has a swelling tendency in the oil domain. Thus, swelling causes an increase in repulsion between the hydrophilic moieties of surfactant, and hence, the surfactant layer curvature becomes more positive. As a result, radius of microemulsion droplet increases [40] and subsequently, interfacial fluidity and droplet surface area increase. Such an increase in interfacial fluidity results in inelastic collisions between droplets, and enhances apparent interdroplet interaction in IPM derived system. At a sufficiently strong interdroplet interaction, the microemulsion droplets stabilized in IPM are less stabilized compared to Hp or Dc oil derived system [41]. Smaller $-\Delta G_t^0$ values were also reported by Hait and Moulik [31] for water/SDS/Bu/IPM system.

Further, Fig. 2 depicts composition dependent $-\Delta G_t^0$ at a fixed ω ($= 20$) for each temperature. An interesting feature, that is, antagonism in $-\Delta G_t^0$ for transfer of Pn ($\text{Pn}_{\text{oil}} \rightarrow \text{Pn}_{\text{int}}$) is evidenced at an equimolar composition of CTAB and Brij-35 (i.e. at $X_{\text{Brij-35}} = 0.5$), whereas synergism in $-\Delta G_t^0$ has been found in the vicinity of equimolar composition (that is, at $X_{\text{Brij-35}} = 0.4$ and 0.6). Very recently, synergistic and antagonistic behaviors were reported in our previous reports for mixed microemulsion systems [5, 33]. Synergism or antagonism in thermodynamic parameters of surfactant mixtures (in micelles or microemulsions) might arise from the non-ideality of surfactant interactions in the confined environment. It was reported earlier that considerable non-ideality shown by ionic/nonionic mixtures is due to the action of the nonionic component that shields the repulsion between charged ionic head groups and, also, due to the attraction between the components, via ion-dipole interactions [42].

However, a plausible explanation for composition dependent synergism or antagonism in ΔG_t^0 can be explained in tune with molecular interactions between CTAB and Brij-35 in mixed micelles put forwarded by Gao et al. [43]. If we consider equimolar composition (that is, $X_{\text{Brij-35}} = 0.5$ or $X_{\text{CTAB}} = 0.5$) of mixed surfactant (CTAB/Brij-35) microemulsions as a reference composition, it can be observed that addition of either CTAB (i.e., at $X_{\text{Brij-35}} = 0.4$ or $X_{\text{CTAB}} = 0.6$) or Brij-35 (i.e., at $X_{\text{Brij-35}} = 0.6$ or $X_{\text{CTAB}} = 0.4$) to an equimolar composition, synergism in $-\Delta G_t^0$ is evidenced at both compositions. It can be argued as follows. The first oxyethylene groups of POE chains (of Brij-35) retard the motion of the trimethyl groups of CTAB due to steric hindrance during the incorporation of Brij-35 in the vicinity of equimolar composition of CTAB/Brij-35 (i.e., at $X_{\text{Brij-35}} = 0.6$). Further, motion of proton near the alkyl ether group of Brij-35 becomes less restricted during the incorporation of CTAB in the vicinity of equimolar composition of CTAB/Brij-35 (at $X_{\text{Brij-35}} = 0.4$), because the trimethyl groups of CTAB separate them apart from each other [43]. Due to these changes in orientation of both CTAB and Brij-35 after addition of both surfactants in the vicinity of equimolar composition may be reflected in the synergism in $-\Delta G_t^0$.

Antagonism in $-\Delta G_t^0$ at equimolar composition at each temperature might be explained in the following manner. The presence of overall lowest concentration of Pn at $X_{\text{Brij-35}} = 0.5$ (i.e., n_a^i as evidenced from Table 1) makes the oil/water interface sterically rigid. As it was reported earlier that increasing alcohol partitioning at the interface, increase the degree of interpenetration of droplets and therefore, increase the interfacial fluidity or flexibility [44]. Rigid conformation of the hydrophobic tails disrupts steric packaging of the interface and leads to partial hydration of the hydrophobic core of CTAB/Brij-35 mixed blends [45]. This partial hydration of the hydrophobic tails at the interface decreases the hydrophobic interactions between the hydrophobic regions of the cosurfactant at the interface, which results in increase in entropy and makes the system more unstable [46]. As a result, CTAB/Brij-35 system shows minima in $-\Delta G_t^0$ at equimolar composition.

Effect of X_{nonionic} and temperature on ΔH_t^0 , ΔS_t^0 , and $(\Delta C_p^0)_t$ of alkanol transfer process

Due to nonlinear dependence of $(\Delta G_t^0/T)$ on $1/T$ in terms of a two degree polynomial equation at each composition ($X_{\text{Brij-35}}$), four values of ΔH_t^0 and ΔS_t^0 at four temperatures

have been evaluated (vide. Fig. S1). Since ΔH_t^0 became a function of temperature, the $(\Delta C_p^0)_t$ values have also been obtained at all compositions from the slope of the plots of ΔH_t^0 vs. T according to Eq. 6. Further, in kinetics and equilibrium studies, an extra thermodynamic linear correlation between ΔH_t^0 and ΔS_t^0 for the involved process is often reported, called the enthalpy-entropy compensation effect, and such a phenomenon has been observed to be valid also for micelle and microemulsion forming systems [25, 32, 33]. A good linear correlation between ΔH_t^0 and ΔS_t^0 has been observed at the temperature of measurement. A comprehension of all these results has been presented in Appendix D, Sec. 3 (Table 1, Figs. S3-S4 and Tables S1-S2).

3.3. Effect of ω and X_{nonionic} on electrical conductivity of mixed surfactant microemulsion

It is known that electrical conductivity can be used to predict qualitatively the interaction between droplets and thus the stability of microemulsion. For example, appearance of an electrical percolation process indicates the existence of large attractive interaction between droplets [47]. In the present report, the dependence of electrical conductivity (σ) on water content (ω) as a function of composition ($X_{\text{Brij-35}} = 0.0 \rightarrow 1.0$) in water/CTAB/Brij-35/Pn/IPM system has been systematically investigated at a fixed surfactant concentration (0.3 mol dm^{-3}) and temperature (303K). The conductivity of the above system was carried out from the appearance of single phase to the phase separation on dilution by water with a fixed surfactant and cosurfactant ratio (1:2, w/w). It can be observed from Fig. S5 (Appendix D) that the single CTAB microemulsion system (at $X_{\text{Brij-35}} = 0.0$) is low conducting and does not exhibit any significant increase in conductivity with increase in ω . This may be due to rigidity of the interfacial film, large molar volume and high viscosity of IPM [48]. Similar observation was also reported earlier for water/AOT/IPM [48] and water/SDS/Pn/IPM microemulsion systems [5]. However, the addition of Brij-35 to the water/CTAB/Pn/IPM system with fixed total surfactant concentration (as mentioned above), a dramatic increase in conductivity has been observed as a function of ω up to equimolar composition ($X_{\text{Brij-35}} = 0.2 \rightarrow 0.5$), beyond which ($X_{\text{Brij-35}} = 0.6 \rightarrow 1.0$) results in a small decrease in conductivity with increasing ω . An in-depth analysis of the results reveals that conductivity increases

slowly with ω and there after a sharp increase is observed at a certain ω for $X_{\text{Brij-35}} = 0.2, 0.4$ and 0.5 blends (Fig. S5). The critical value for sharp linear enhancement in conductivity (σ) with the addition of water is considered as percolation threshold point [5]. The critical value of ω for $X_{\text{Brij-35}} = 0.2, 0.4$ and 0.5 has been found to be $\omega \leq 27.57, \omega \leq 34.83$ and $\omega \leq 39.05$, respectively. Similar observation was also evidenced in our previous report for water/SDS/Brij-35/Pn/IPM microemulsion systems [5]. The details of these results have been delineated in Appendix D, Sec. 4.

3.4. Droplet dimension of single and mixed surfactant microemulsions by DLS studies

The droplet size (hydrodynamic diameter, D_h) and the size distribution in w/o single and mixed (CTAB/Brij-35) surfactant microemulsions have been measured by employing the DLS technique and subsequently, analyzed in terms of count rate and polydispersity index (PDI) of the droplets [49, 50]. The results are presented in Tables 3A and 3B. The similar compositions of w/o mixed surfactant microemulsions were chosen for DLS measurements, as those were used in dilution experiments as function of X_{nonionic} ($X_{\text{Brij-35}} = 0.0 \rightarrow 1.0$) and ω ($= 20, 25, 30, 35, 40$ and 45) at a constant temperature of 303K . It can be observed from the Tables 3A and 3B that D_h values of the microemulsion droplets increase remarkably from 10.92 nm to 18.91 nm in IPM with the increase in proportion of nonionic surfactant ($X_{\text{Brij-35}} = 0.0 \rightarrow 1.0$) in the mixed systems, whereas about 1.5 folds decrease in droplets count rate has been observed under the prevailing condition (Table 3A). The decrease in droplets count rate indicates that the total number of microemulsion droplets decreases with increasing the content of Brij-35. Similar trend was observed in our previous report for water/SDS/Brij-35/Pn/IPM microemulsions and explained therein [5].

Furthermore, a comparative study of D_h values obtained for mixed CTAB/Brij-35 (herein, presented) and SDS/Brij-35 systems [5] reveals that, D_h for former system at comparable conditions in IPM (9.80 nm to 18.91 nm at $X_{\text{Brij-35}} = 0 \rightarrow 1.0$ and 14.55 nm to 27.63 nm at $\omega = 20 \rightarrow 40$). This can be argued as follows. It is evident from Table 1 that, n_a^i for CTAB/Brij-35 systems is lower compared to SDS/Brij-35 systems [$(19.08$ to $40.50) \cdot 10^{-4}$ mol and $(12.41$ to $51.11) \cdot 10^{-4}$ mol at $\omega = 20 \rightarrow 40$ and $X_{\text{Brij-35}} = 0 \rightarrow 1.0$, temperature =

293→323K, respectively] at comparable conditions in IPM [5]. Pn molecules are mainly located at the interface layer and oil phase due to their negligible solubility in water [25].

Table 3(A). Hydrodynamic diameter (D_h) and count rate of water droplets in w/o mixed surfactant microemulsion at fixed water content ($\omega = 20$) and temperature (303K).^a

System: water/CTAB/Brij-35/Pn/IPM							
$X_{\text{Brij-35}}$	0.0	0.2	0.4	0.5	0.6	0.8	1
D_h/nm	10.92	12.32	13.97	15.67	16.78	17.63	18.91
Count Rate/kcps	91.80	85.80	79.10	73.20	67.70	64.30	61.50

(B) Hydrodynamic diameter (D_h) and count rate of water droplets in w/o mixed surfactant microemulsion with increase in water content ($\omega = 20 \rightarrow 40$) and fixed $X_{\text{Brij-35}}$ (0.5), temperature (303K).^a

System: water/CTAB/Brij-35/Pn/IPM							
ω	20	25	30	35	40	45	
D_h/nm	15.67	19.26	24.10	28.52	32.07	36.44	
Count Rate/kcps	73.20	62.40	51.90	41.40	33.70	25.10	

^a All the mixed microemulsion systems are formed using constant amount of mixed surfactant (0.5 mmol) and oil (14.0 mmol).

The total interface area becomes larger as more Pn molecules are incorporated at the interfacial layer. An increase in the interface area causes the number of droplets to increase and the droplet size to shrink [51]. Similar observation was also reported earlier by Zhang et al. [52] for water/AOT/Pn/IPM systems.

3.5. State of water of single and mixed surfactant microemulsions from FTIR studies

In principle, the time scale of FTIR is short enough to detect different types of water species in w/o microemulsion, provided that the difference in vibrational energy is suitably large [14, 53, 54]. Further, the use of HOD molecule as a probe has been shown to be advantageous, as the O-D band is decoupled from the O-H band and appears in a

region (2200 cm^{-1} to 2800 cm^{-1}) which is comparatively free from other strong absorption[14, 54, 55]. According to our previous report[26], a small amount of D_2O (10%) was mixed with H_2O , so that a rapid exchange between H and D atoms takes place, which led to the formation of HOD molecules. The O–D stretching band of these molecules reflects only the H-bonding interactions between water molecules. Thus, the intramolecular interactions between the two OH (or OD) oscillators in H_2O (or D_2O) molecules do not complicate the O–H (O–D) stretching band contour as observed for pure water [26, 56]. The isotopic solution of 10% $\text{D}_2\text{O}/\text{H}_2\text{O}$ mixture was chosen for the formulation of w/o mixed microemulsion [26, 57]. The FTIR techniques have been employed to explore the possibility of alteration of water structure due to change in the micellar characteristics viz. size, interfacial configuration with the variation of composition, $X_{\text{Brij-35}}$ ($= 0.0 \rightarrow 1.0$) at a fixed water content ($\omega = 20$) and surfactant-cosurfactant mass ratio ($= 1:2$) at 303K.

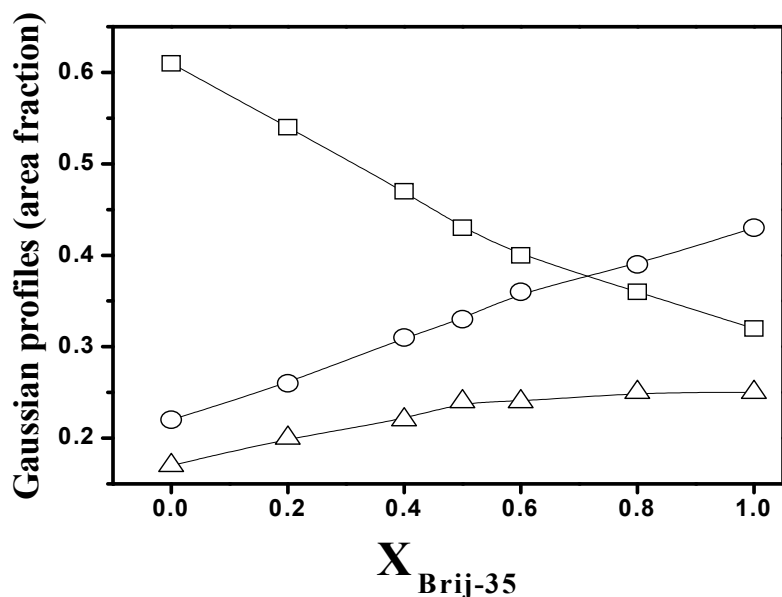


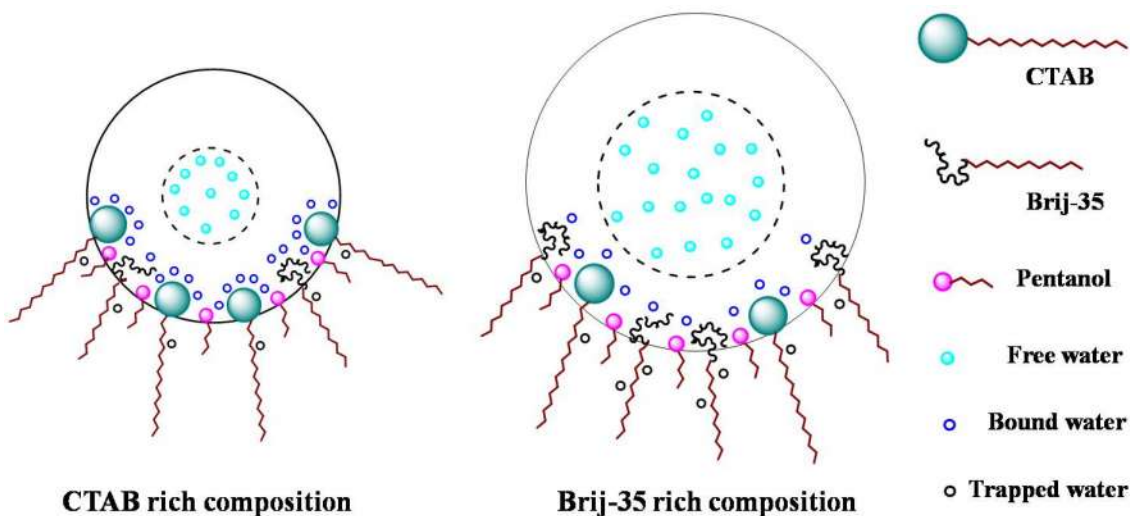
Fig. 3. The variation of Gaussian profiles (area fraction) of the normalized spectra of different water species (free: open circle, bound: open square and trapped: open triangle) as a function of $X_{\text{Brij-35}}$ at a fixed $\omega (= 20)$.

We focus our attention in the $2200\text{--}2800\text{ cm}^{-1}$ frequency window, which is considered as a fingerprint region for the vibrational stretch of O–D bonds in water [58, 59]. It has been

reported that water exists in three ‘states’ or ‘layers’ in w/o microemulsions from FTIR measurement [60, 61], although report on four-component hydration model, viz. free, anion-bound, bulk like and cation-bound water are available in literature from FTIR and NMR measurements [27, 62]. In the present study, the peaks corresponding to O-D bonds have been fitted as a sum of Gaussian bonds with the help of Gaussian curve fitting program. The vibrational characteristics, particularly the peak area corresponding to each peak, and other results have been analyzed using three-state models to unravel the different types of water species inside the nanopool. According to three states model, the solubilized water in microemulsions can be identified as free water, bound water and trapped water molecules and a representative result of deconvolution is depicted in Figs. S6A, S6B, S6C (Appendix D). The free water molecules, occupying the cores of water pool of w/o microemulsions, possess strong hydrogen bonds among themselves that means they have properties similar to bulk water. Such H-bond shifts the O-D stretching band towards lower frequency at about 2450 cm^{-1} (Figs. S6A-S6C) [14, 60, 61]. The bound water viz. the surfactant head group bound water molecules resonates in the mid frequency region and the IR peak appears at about 2550 cm^{-1} (Figs. S6A-S6C) [14, 60, 61]. Apart from these water species, there are water molecules dispersing among long hydrocarbon chains of surfactant molecules termed as trapped water molecules [27, 60, 61]. This type of water exists as monomers (or, dimers) and free from hydrogen bonding interaction with its surroundings. As trapped water molecules are matrix-isolated dimeric or monomeric in nature, they absorb in the high frequency region at about 2650 cm^{-1} (Figs. S6A-S6C) [27, 60, 61]. The relative abundance [Gaussian profiles (area fraction)] of different water species (viz. free, bound and trapped water) as a function of $X_{\text{Brij-35}}$ (= 0.0→1.0) has been shown in Fig. 3 [26, 60, 63].

With the progressive inclusion of nonionic Brij-35 (= 0.0→1.0) at the interface, the abundance of free water increases while the population of bound water gradually decreases under the prevailing condition (Fig. 3 and Scheme 1). It is noteworthy to mention that the increase in nonionic surfactant content results in decrease of the total hydration capacity of the polar headgroups of the mixed surfactants [15]. Consequently,

the relative abundance of free water gradually increases with increasing $X_{\text{Brij-35}}$ (= 0.0→1.0) (Scheme 1) [16, 64].



Scheme 1. Change of state of water with increase in water content in water/CTAB/Brij-35/Pn/IPM microemulsions.

As a result, the physicochemical characteristics of the encapsulated water in confined environment show a linear effect of mixing of surfactants at the interface. Interestingly, it is apparent from DLS measurements that modification of different water states (bound and free water molecules) in confined environment eventually occur with the swelling of the droplet size ($D_h = 10.92 \text{ nm} \rightarrow 18.91 \text{ nm}$) with increasing proportion of $X_{\text{Brij-35}}$ (= 0.0→1.0) at a fixed water content ($\omega = 20$) (Scheme 1). Similar observation with respect to free and bound water was reported for water-in-hydrocarbon oil (Hp or Dc or i-Oc) microemulsions stabilized by mixed AOT/Brij-30 [16], C_n TAB/Brij-58 ($n = 12 \rightarrow 18$) [26], and Brij-58/CTAB [63]. In addition, the population corresponding to the trapped water molecules shows only a marginal variation (or an overall weak increasing tendency with both interfacial stoichiometry as well as droplet size) (Fig. 3). It, therefore, emerges that the nature of the interface as well as the size of the droplets have major impacts on the water hydrogen bond network dynamics regardless of the nanoscopic confinement of water in IPM oil derived w/o microemulsion [26, 63-65]. To further substantiate present

observations, SANS or ^1H NMR rotating frame nuclear Overhauser effect spectroscopy (ROSEY) studies and ultrafast dynamics (picosecond or femtosecond spectroscopy) of confined water molecules in these systems needs to be explored in subsequent studies.

3.6. Evaluation of chemical shift for various components of water (^1H NMR spectroscopic technique followed by mathematical evaluation)

The microstructure of solubilized water in w/o microemulsion has been studied extensively in the past using FTIR and ^1H NMR spectroscopic techniques. The states and structure of the solubilized water in reversed micelles and microemulsions of AOT and of NaDEHP (in Hp) using FT-IR and NMR spectroscopic parameters have been reported [27, 62]. Recently, Bumajdad and coworkers have studied the structure of water, solubilized by reverse aggregates of mixtures of DDAX/DTAX ($X = \text{Br}^-$ or Cl^-) in Hp by same noninvasive techniques viz., ^1H NMR and FT-IR [14]. Herein, we focus on the study of solubilized water structure in w/o water/CTAB/Brij-35/Pn/IPM (S: CS = 1: 2) mixed microemulsions, by combining the results of FTIR and ^1H NMR spectroscopic measurements [27].

As reported earlier, different types of water species coexist and exchange rapidly in w/o microemulsion systems. The exchange rate is faster than NMR frequency and, therefore, the observed value of water proton magnetic resonance is the weighted average of the components contributed by various water species [27, 62]. In the present study, a simple mathematical equation, as proposed by Zhou et al. [27], has been used to evaluate the chemical shift of individual components of different water species present in w/o microemulsion system is given below,

$$\delta = X_{\text{free}}\delta_{\text{free}} + X_{\text{bound}}\delta_{\text{bound}} + X_{\text{trapped}}\delta_{\text{trapped}} \quad (7)$$

The evaluation is based on the fact that the chemical shift of water protons in w/o mixed microemulsion is considered as the weighted average of those of the individual components [27].

The chemical shifts of individual components of different water states viz. δ_{free} , δ_{bound} , and δ_{trapped} can be evaluated by inserting the observed δ values and corresponding area fractions, X_{free} , X_{bound} and X_{trapped} into Eq. (7). The area fraction of individual components has been adopted as estimated from FTIR measurements [27]. In order to evaluate the chemical shifts of individual components of different water species, three different

observed δ values as well as the formation of three simultaneous equations are required for solving Eq. (7) [27]. Hence, we have selected three different compositions of w/o mixed surfactant microemulsion as a function of X_{nonionic} ($= 0.0, 0.2$ and 0.4) for ^1H NMR study. $X_{\text{nonionic}} = 0.0$ represents pure (or single) CTAB system, whereas $X_{\text{nonionic}} = 0.2$ and 0.4 represent mixed CTAB/Brij-35 systems.

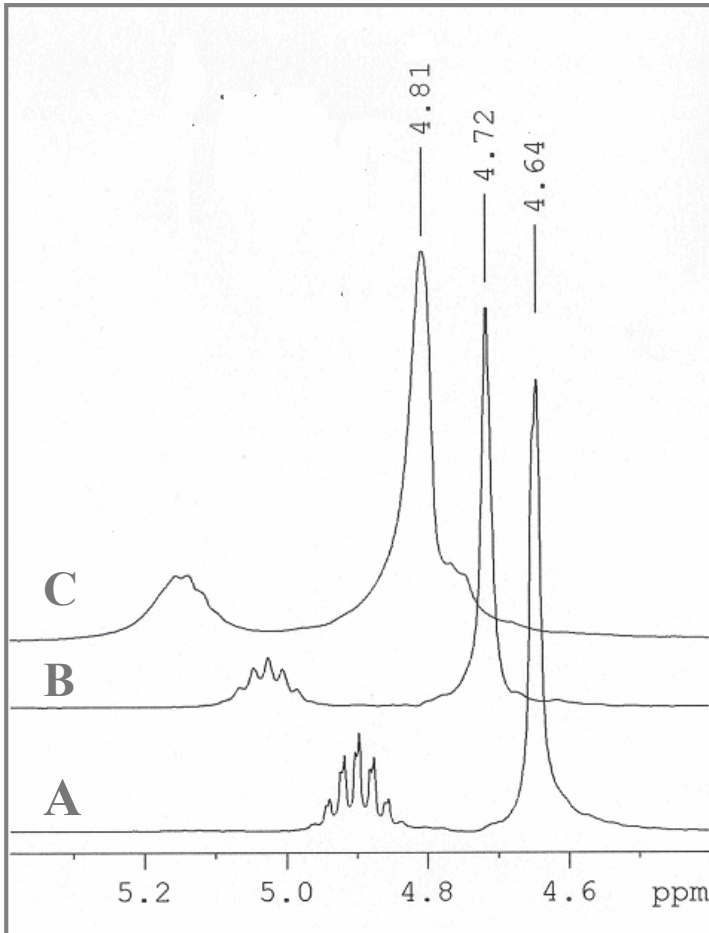


Fig. 4. ^1H NMR peak of water protons in w/o CTAB/Brij-35/Pn/IPM systems as function of $X_{\text{Brij-35}}$ at a constant ω ($= 20$) (A; $X_{\text{Brij-35}} = 0.0$, B; $X_{\text{Brij-35}} = 0.2$, C; $X_{\text{Brij-35}} = 0.4$).

The single peaks in ^1H NMR spectra of the solubilized water in w/o mixed microemulsion systems indicate the rapid exchange between water protons at various states (Fig. 4). So, the Eq. (7) can be written as follows [27],

$$4.64 = 0.22 \delta_{\text{free}} + 0.61 \delta_{\text{bound}} + 0.17 \delta_{\text{trapped}} \quad (8)$$

$$4.72 = 0.26 \delta_{\text{free}} + 0.54 \delta_{\text{bound}} + 0.20 \delta_{\text{trapped}} \quad (9)$$

$$4.81 = 0.31 \delta_{\text{free}} + 0.47 \delta_{\text{bound}} + 0.22 \delta_{\text{trapped}} \quad (10)$$

The evaluation of the three simultaneous Eqs. (8)- (10) showed the existence of three individual components of water species inside the pool and the calculated chemical shift of individual components i.e. δ_{free} , δ_{bound} and δ_{trapped} appears at 5.76, 4.20 and 4.77 ppm, respectively. A similar δ_{bulk} value (= 5.68 ppm) was reported earlier for water/AOT/Hp w/o microemulsion systems [27]. However, δ_{bound} value does not match closely with the present system and the result possibly reflects the influence of type and size of the polar head group of major surfactant (CTAB) and content of the auxiliary surfactant, Brij-35 on the microenvironment [27]. The ^1H NMR spectroscopic measurement followed by mathematical evaluation supports the existence of three different types of water species in these systems. Further, it is evident from Fig. 4 that observed δ values of ^1H NMR spectra for the solubilized water in the present systems shifted towards downfield (4.64 ppm \rightarrow 4.81 ppm) with the addition of nonionic surfactant, X_{nonionic} (= 0.0 \rightarrow 0.4). These observations corroborate well with the results of FTIR, wherein free water exhibits a lower stretching frequency (2450 cm^{-1}) and responds to a lower resonance position. The addition of nonionic surfactant enhances the stretching frequency (2550 cm^{-1}) responding to a higher resonance position which indicates the presence of free of water species [61]. However, further studies involving w/o mixed surfactant cationic or anionic/nonionic microemulsions are warranted in this direction.

3.7. Antimicrobial activity in single and mixed surfactant microemulsions

In this section, the effect of individual constituents of the microemulsion systems, water/CTAB/Brij-35/Pn/IPM on antimicrobial activity has been examined against the bacterial strains, gram-positive - *B. subtilis* and gram-negative - *E. coli* at 303K prior to work on the microemulsion formulations and the results are presented in (Table S3). It is evident from Table S3 that CTAB exhibits considerable antimicrobial activity at different concentrations (0.5 \rightarrow 0.1 mmol) comparable to concentration of CTAB, i.e., [CTAB] contained in each composition of microemulsions, $X_{\text{Brij-35}} = 0.0 \rightarrow 0.8$, whereas Pn and Brij-35 show insignificant antimicrobial activity against both strains [66, 67]. IPM did not show antimicrobial activity at all. Such report is also available in literature [68]. Of all the constituents, the best inhibitory effect was produced by aqueous CTAB i.e., at [CTAB] = 0.5 mmol, and the resultant diameter of inhibition zones (diz) was found to be

12 mm and 10 mm for *B. subtilis* and *E. coli*, respectively. Further, inhibitory effect of aqueous CTAB decreases with decrease in concentration against both bacterial strains. Subsequently, antimicrobial activity of the microemulsion formulations have been examined as a function of composition of mixed surfactants [$X_{\text{Brij-35}} = 0.0 \rightarrow 1.0$, S/CS= 1:2 (w/w)] at 303K, against the matching strains, *B. subtilis* and *E. coli* bacteria and the results are presented in Table S4 and Fig. S7 (Appendix D). Moreover, comparative antimicrobial activity (or, effectiveness) of the microemulsion formulations has also been depicted in Table S4, assuming the efficiency of the ingredient shown to be unity as the best inhibitor (herein, aqueous [CTAB] equals to 0.5 mmol). It can be seen from (Table S4) that the d_{50} values and effectiveness of the microemulsion formulations as a function of $X_{\text{Brij-35}}$ ($= 0 \rightarrow 1$) did not follow a linear course against the bacterial strains. Interestingly, microemulsions at mixed surfactant compositions, ($X_{\text{Brij-35}} = 0.2$ to 0.8) demonstrate better antimicrobial activity or effectiveness than pure surfactants, ($X_{\text{Brij-35}} = 0$ and 1.0) with maximization at compositions, $X_{\text{Brij-35}} = 0.4$ and 0.6 . The resultant d_{50} values and effectiveness of the microemulsion formulations were found to be 18 mm, 1.50; 17 mm, 1.42 and 15 mm, 1.50; 14 mm, 1.40 for *B. subtilis* and *E. coli* respectively. Hence, reported w/o microemulsions at mixed surfactant compositions could be prospective for using with good standing of antimicrobial property. However, pure nonionic microemulsion (Brij-35/Pn/IPM/water at $X_{\text{Brij-35}} = 1.0$) exhibits considerable antimicrobial activity (Table S4), in spite of negligibly small antimicrobial activity shown by Brij-35 or Pn alone, and IPM did not shown any activity (Table S3). Recently, Anjali et al. [69] reported that water/Tween-20/refined sunflower oil microemulsion possesses superior antimicrobial activity against the bacterial pathogens, *E. coli*, *S. aureus* and *P. aeruginosa* than refined sunflower oil or Tween 20 as individual component using agar well diffusion assay, and spread plate method. The difference in antimicrobial activity between the individual constituents and microemulsion system may be due to different types of interactions between the microemulsion droplets and bacterial membranes which significantly decreased hydrophobicity of the bacterial cell, leading to rapid loss of bacterial viability [70].

Further, the absolute d_{50} values have been found to be lowered against gram-negative bacteria (*E. coli*) than gram-positive bacteria (*B. subtilis*) for each composition as well as

the individual constituents of the microemulsion formulations (Table S3 and S4). It may be due to variation in lipid content of the cell membranes in both bacterial pathogens, which results in higher resistance towards antimicrobial properties of former templates than later [66].

Nevertheless, the diffusion of the microemulsion systems in the media (nutrient agar) was examined by the dye encapsulation method (viz. methylene blue at $10^{-3} \text{ mol dm}^{-3}$ as a function of system composition, $X_{\text{Brij-35}} = 0.0 \rightarrow 1.0$, to ascertain the role of diffusion, if any. No such variation in diffusion was observed in these systems. Hence, it can be inferred that the diffusion is not a pivotal factor behind the antimicrobial activities of the mixed microemulsions.

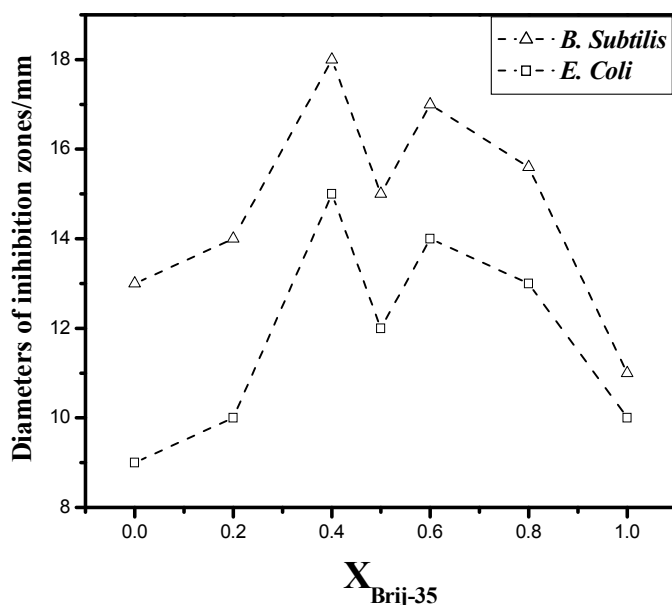


Fig. 5. Antimicrobial activity (diameters of inhibition zones) in water/CTAB/Brij-35/Pn/IPM microemulsions as a function of composition, $X_{\text{Brij-35}}$ ($= 0.0 \rightarrow 1.0$) at fixed water content ($\omega = 20$) and temperature (303K).

However, a correlation between composition dependence of antibacterial activity on the growth of both bacterial strains with the spontaneity of formation vis-à-vis thermodynamic stability of the microemulsion systems is exhibited in prevalent condition (Fig. 5). Both the plots resemble each other. It is clearly evident that the mixed microemulsions show synergism in free energy of formation ($-\Delta G_t^0$) at $X_{\text{Brij-35}} = 0.4$ and

0.6 (vide. Sec. 3.2.2), wherein the highest antimicrobial activity has been observed. From close scrutiny of Fig. 5, it can be seen that comparatively lower antimicrobial activity has been evidenced at equimolar composition [$X_{\text{Brij-35}} = 0.5$, which corresponds to preceding and forwarding compositions (i.e, $X_{\text{Brij-35}} = 0.4 \rightarrow 0$ or $X_{\text{Brij-35}} = 0.6 \rightarrow 1.0$, respectively)], where antagonism in $-\Delta G^0$ has also been observed (Fig. 2). In other words, these results can be explained from Table S4 as follows: it can be observed that absolute ΔG^0 values increases (13.0 \rightarrow 18.0) by the addition of Brij-35 at CTAB rich compositions ($X_{\text{Brij-35}} = 0 \rightarrow 0.4$), whereas it also increases (11.0 \rightarrow 17.0) by the addition of CTAB at Brij-35 rich compositions ($X_{\text{Brij-35}} = 1.0 \rightarrow 0.6$). It seems that departure from these two trends in ΔG^0 values against the composition (as mentioned above) occurs at equimolar composition ($X_{\text{Brij-35}} = 0.5$). It may be due to rigid conformation of the hydrophobic tails of amphiphiles, which disrupts steric packaging of the interface due to less partitioning of alcohol at the interface, which has already been discussed in Sec. 3.2.2.

Reports are available in literature on antimicrobial action of the microemulsions (involving nonionic surfactant) against several bacterial pathogens from different aspects [19, 69-71]. However, further experimentation [for example, thermodynamic stability studies (centrifugation study, heating-cooling cycle, freezing-thaw cycle, kinetic stability), kinetics of killing organisms, assessment of morphological alterations in cell membrane by scanning electron microscopy (SEM) etc.] is required to give insight on the mode of action of antimicrobial activity of the characterized mixed surfactant microemulsion systems, which is beyond scope of the present report.

4. Conclusion

In the present work, we report on the characterization of water-in-biocompatible oil (IPM) microemulsions stabilized by mixed surfactants, CTAB/Brij-35 and Pnat different compositions of surfactants and physicochemical conditions by employing phase studies, dilution method and conductivity, DLS, FTIR and ^1H NMR techniques. In addition, antimicrobial activity of these systems (including individual components) has been examined against the bacterial strains *B. subtilis* (gram-positive) and *E. coli* (gram-negative). Phase study reveals a considerable amount of single phase (1 ϕ) clear microemulsion region for mixed systems at a fixed surfactant-cosurfactant ratio (= 1:2) and constant temperature (303K). The mixed surfactant composition ($X_{\text{Brij-35}} = 0.0 \rightarrow 1.0$)

influences area of single phasic clear microemulsion zone. Synergism in interfacial composition (n_a^i or n_a^i/n_s) has been observed at ω equals to 35 and subsequently, decreases up to $\omega = 45$. Physicochemical (molecular) interactions among the constituents [amphiphiles (viz. Brij-35, CTAB and Pn) and water] in the microenvironment of the systems might be responsible for the threshold level of stability at $\omega = 35$. The transfer process of alkanol ($Pn_{oil} \rightarrow Pn_{int}$) or formation of microemulsions has been found to be spontaneous at all compositions ($X_{Brij-35} = 0.0 \rightarrow 1.0$) in the ranges of ω ($= 20 \rightarrow 45$) as well as of temperature ($293K \rightarrow 323K$). Synergism in $(-\Delta G_t^0)$ for Pn transfer process ($Pn_{oil} \rightarrow Pn_{int}$) has been observed in the vicinity of equimolar composition ($X_{Brij-35} = 0.4$ and 0.6), whereas antagonism exhibits at equimolar composition ($X_{Brij-35} = 0.5$). The overall transfer process is exothermic with negative entropy change (i.e., ordered) at all experimental temperatures in IPM for single CTAB or Brij-35 system. The overall mixed compositions (i.e. at $X_{Brij-35} = 0.2 \rightarrow 0.8$) have been ended up with absorption of heat with disordered state or release of heat with ordered state, depending on composition ($X_{Brij-35}$) and thermal condition. Both ΔH_t^0 and ΔS_t^0 values decrease with increase in temperature at mixed compositions and also compensate with each other with fair degree of linearity (average value of correlation of coefficients equals to 0.9980). A dramatic increase in conductivity has been observed as a function of ω up to a composition range ($X_{Brij-35} = 0.2 \rightarrow 0.5$), beyond which ($X_{Brij-35} = 0.6 \rightarrow 1.0$) conductivity decreases with increasing ω at 303K. DLS measurements show a linear increase in droplet size as a function of both ω and composition ($X_{Brij-35} = 0.0 \rightarrow 1.0$) at 303K. The O-D stretching vibration of HOD solubilized in w/o mixed surfactant (CTAB/Brij-35) microemulsions as obtained from FTIR measurements in the $2200-2800 \text{ cm}^{-1}$ frequency window reveals the existence of three different types of water molecules viz. free or bulk type, bound and trapped inside the pool. With the progressive inclusion of Brij-35 ($X_{Brij-35} = 0.0 \rightarrow 1.0$) at the interface, the abundance of free water increases while the population of bound water gradually decreases under the prevailing condition. Further, FTIR study indicates that the composition of the interface as well as the size of the droplets have major impacts on water hydrogen bond network dynamics regardless of the nanoscopic confinement of water in these systems [64, 65]. 1H NMR spectroscopic measurements followed by mathematical evaluation also support the existence of three different types of water

species in the pool of these systems[27]. Water/CTAB/Brij-35/Pn/IPM microemulsions at mixed compositions ($X_{\text{Brij-35}} = 0.2-0.8$) at 303K demonstrate higher antimicrobial activity against both bacterial strains compared to individual constituents (i.e., CTAB or Brij-35 or Pn) of microemulsions at 303K at similar conditions. However, single Brij-35 system ($X_{\text{Brij-35}} = 1.0$) exhibits considerable antimicrobial activity, in spite of negligibly small antimicrobial activity shown by Brij-35 or Pn alone. IPM did not show any activity. Further, *E. coli* exhibits somewhat more resistance than *B. subtilis* towards each composition as well as the individual constituents of the microemulsions. These w/o microemulsions at mixed surfactant compositions could be prospective for using with good standing of antimicrobial property. Moreover, these systems mixed surfactant w/o microemulsions could be employed for applications in different processes like solubilization, catalysis of chemical reactions [8, 9], and size and polydispersity of nanomaterial synthesized in microemulsion in a more effective and convenient way [10, 72]. Further, the dynamic mass transfer phenomenon across the interface with variation in content of Brij-35 ($X_{\text{Brij-35}}$), as evidenced from conductivity measurement, might be useful in petroleum-processing technologies [73]. Composition-dependent temperature insensitive microemulsions could be prospective to employ as decontamination media for toxic industrial chemicals and chemical weapons as well, because it undergoes several temperature changes without time for relaxation during the decontamination process [73].

References

References are given in BIBLIOGRAPHY under Chapter VI (pp. 250-253).